STP 1580, 2015 / available online at www.astm.org / doi: 10.1520/STP158020140081

Christine Sidoroff,[1] Michel Perez,[2] Pierre Dierickx,[1]
and Daniel Girodin[1]

Advantages and Shortcomings of Retained Austenite in Bearing Steels: a Review

Reference

Sidoroff, Christine, Perez, Michel, Dierickx, Pierre, and Girodin, Daniel, "Advantages and Shortcomings of Retained Austenite in Bearing Steels: a Review," *Bearing Steel Technologies: 10th Volume, Advances in Steel Technologies for Rolling Bearings*, STP 1580, John M. Beswick, Ed., pp. 312–348, doi:10.1520/STP158020140081, ASTM International, West Conshohocken, PA 2015.[3]

ABSTRACT

Bearing steels are heat treated to get martensitic microstructures providing high hardness necessary for good rolling contact fatigue performance. Without specific action taken, austenite is generally retained after heat treatment in the final component with a more or less important content. Depending on the requirements of each application, retained austenite can be desired because of beneficial effects such as improvement of rolling contact fatigue performance, mostly in contaminated lubricating conditions, or can be avoided if dimensional stability is needed for example in cases of bearings operating for long times at high temperatures. Because bearing steels are subjected to more and more demanding operating conditions, heat treatments and microstructures are engineered in terms of retained austenite in order to use the beneficial effect of a stabilized retained austenite, or on the contrary to suppress retained austenite. This paper discusses the advantages and shortcomings of retained austenite in bearing steels, with illustrations of work realized in NTN-SNR.

Keywords

bearing steel, 100Cr6, SAE 52100, retained austenite, dimensional stability, carbonitriding, contaminated lubrication

---

Manuscript received July 7, 2014; accepted for publication October 10, 2014; published online November 26, 2014.

[1] NTN-SNR Roulements, Technology and Innovation Dept., Materials Laboratory E2M, Annecy, France.

[2] Univ. Lyon, INSA Lyon, MATEIS, UMR CNRS 5510, Villeurbanne, France.

[3] ASTM 10th International Symposium on *Advances in Steel Technologies for Rolling Bearings*, on May 6–7, 2014 in Toronto, Ontario, Canada.

Introduction

Bearings in service must meet more and more demanding requirements in terms of load, temperature or complex loading, but the first and more important requirement of all is to present long service lives under rolling contact fatigue conditions without failure, and that means in terms of materials properties a minimum hardness of 58 HRC for rolling contact fatigue resistance (in conjunction with the appropriate inclusion cleanliness) [1], and a good wear resistance.

This is obtained by the appropriate choice of steel grade, steelmaking process route, and heat treatment.

If no specific requirements such as structural fatigue or impact resistance are expressed, through-hardened steels are used, such as SAE 52100 steel in case of standard temperature conditions (hereafter mentioned as standard bearing steels). If application temperatures are too high for standard bearing steels, alloyed steels presenting secondary hardening properties such as M50 can be selected (hereafter mentioned as high temperature steels).

Another important feature that bearing steels must retain in service all through the life of the mechanical component is the initial internal clearance of the bearing, and its interference with the surrounding parts. Therefore the size change must be limited at the service temperature for standard bearing steels by selecting the appropriate heat treatment, and be non-existent for high temperature steels.

Steels such as SAE 52100 are easily hardened to the required level, by austenitizing at temperatures above AC_1, quenching, and tempering. The metallurgical structures obtained after hardening are metastable and will evolve in service towards more stable states, resulting in size changes or dimensional instability.

The reasons for this dimensional instability are well known and have been documented since the 1940s in many publications [2–10], and the culprit always designated is a metastable phase remaining in quenched high-carbon alloyed steels microstructure, retained austenite.

Retained austenite is a metastable phase that decomposes under thermal or mechanical stresses, and this specific phenomenon can be an asset for bearings in some cases, or be detrimental because of the size changes it produces, acting as a “friend” or as a “foe” as it was well discussed in a publication from 1994 entitled “Retained austenite: new look to an old debate” focused on gears [11].

Twenty years later, the aim of this paper is to review work realized in NTN–SNR and in the literature, to provide “a newer look to an older debate,” as far as it is still an issue of discussion in the academic and industrial community.

The metallurgical mechanisms behind the instability are slightly more complex than it seems and are described in the Shortcomings section below. Dimensional stability of many bearing steels, or better said, instability, has been extensively studied in NTN–SNR since the 1960s [12–14]. The latest study performed on SAE 52100 aimed at understanding the relative contributions of the different phenomena in order to predict dimensional variations occurring during service. This work is detailed in the Shortcomings section.

In some cases, retained austenite, depending on its intrinsic properties and localization in the microstructure, improves the rolling contact fatigue (RCF) performance under severe lubrication conditions [15–20]. This feature of retained austenite is discussed in the Advantages section, through the description of two material solutions developed in NTN–SNR: a through-hardened modified SAE 52100 and carbonitrided SAE 52100.

The fourth section of the paper presents a review of how it is possible to influence the retained austenite content and its stability, to design a solution depending on the requirement of the application: either a dimensionally stable steel (no retained austenite, or a limited retained austenite content), or a damage tolerant steel.

Shortcomings of Retained Austenite: Dimensional Instability

FROM METALLURGICAL PHENOMENA TO DIMENSIONAL VARIATIONS

Tempering of steels has been extensively studied in the literature [21,22]. After austenizing and quenching, the microstructure of high carbon (alloyed) bearing steels is mainly martensitic and composed of the following constituents: carbon oversaturated martensite, retained austenite because the martensite start (M_S) and finish (M_F) temperatures are low enough (M_F below room temperature) to retain austenite, and alloyed carbides, not fully dissolved during austenizing (hereafter called undissolved carbides). These two first constituents, martensite and retained austenite, are metastable and evolve in service towards a more stable state.

Martensite tempering is often described using the following stages associated with temperature ranges in which they are likely to take place [21,22]. These phenomena can happen at lower temperatures, provided time is left for these transformations to occur.

Martensite is a supersaturated metastable phase retaining the parent phase (austenite) carbon concentration.

Stage 0: ($T < 100°\text{C}$)

Carbon atoms segregate to dislocations. Up to 0.2 wt. %C can be involved in atmospheres on dislocations.

Stage 1: ($100 < T < 200°\text{C}$) $\alpha' \rightarrow \alpha'' + \varepsilon$

Oversaturated martensite rejects carbon, creating metastable nonstoichiometric ε-carbides ($Fe_{2,4}C$).

Stage 2: ($200 < T < 300°\text{C}$) $\gamma_R \rightarrow \alpha + Fe_3C$

Retained austenite, also a metastable phase, decomposes into a mix of ferrite and cementite (Fe_3C).

Stage 3: ($250 < T < 350°\text{C}$) $\alpha'' + \varepsilon \rightarrow \alpha + Fe_3C$

Carbon precipitates from impoverished martensite to form cementite carbides (Fe_3C, also referred to as θ in this paper), to the detriment of ε-carbides.

Stage 4: ($T > 350°C$)

Carbides coarsen and sphereodize. The structure is subjected to recovery, and then recristallization.

To summarize, two different phenomena occur during the first stages of tempering: precipitation of carbides from martensite (impoverishment of the carbon-supersaturated martensite and subsequent formation of carbides), and transformation of retained austenite.

Those phase evolutions and transformations produce macroscopic dimensional variations [5,23,24].

Precipitation From Martensite

Martensite has a tetragonal lattice, and its parameters are dependent on carbon concentration [25].

When carbon is rejected from martensite and carbides precipitate, two opposite effects take place:

- Contraction of the martensite because of lattice size reduction (tetragonal loss and volume reduction of lattice cell).
- Slight expansion because of carbide formation, not high enough to compensate the contraction previously mentioned.

These two effects result in a continuous contraction, as long as carbon precipitates into ε-carbides, and Fe_3C carbides.

In his extensive review on bearing steels, Bhadeshia [24] reports a work from Averbach [2] stating that ε-carbides precipitation causes negligible contraction strains of about 10^{-4} between 50 and 150°C.

Other works present shrinkage caused by ε-carbide precipitation of -0.18 % for a 1.1 wt. %C alloy [25], or -0.2 % for 1 wt. %C alloys [23].

Transformation of Austenite

Austenite has a face-centered cubic (fcc) structure, which is the densest existing structure, so that when it transforms into ferrite and cementite, the volume increases [24].

Bhadeshia reports a volume expansion, with some compensation due to shrinkage in case of concomitant Fe_3C precipitation, of 10^{-3} per % of decomposed retained austenite.

Luty [9] states that retained austenite decomposition can produce an expansion of 4 μm for 100 mm.

Moreover, the dilatation reported by Roberts [23] associated with the decomposition of retained austenite is $+1.1$ %.

Peilloud [12] presents an estimation of 15 μm dilatation by % of decomposed retained austenite for a component with a 100 mm diameter.

Fourth Stage

Carbide coarsening and spheroidizing, recovery, and recristallization result in a macroscopic contraction, rarely referred to in technical publications.

In the end, for an as-quenched martensite, the dimensional evolution when subjected to a temperature-time cycle will present successively a contraction caused by carbon rejection and ε-carbide precipitation, then an expansion caused by austenite decomposition, partially compensated by cementite precipitation, then again a contraction due to the end of cementite precipitation, and with a slight change in slope a contraction caused by the structure evolutions during the fourth stage.

FROM THE EVALUATION OF INDIVIDUAL CONTRIBUTIONS OF EACH PHENOMENON TO THE PREDICTION OF MACROSCOPIC DIMENSIONAL VARIATIONS

The investigation of microstructure evolution during tempering and service (both stages can be considered as a thermal ageing realized after quench), can be studied using many different techniques: characterization techniques such as electron microscopy to identify microstructure constituents [26], and macroscopic measurements such as internal friction [27], resistivity [28], or dimensional and thermal analysis [23,25] can help to qualify the microstructural evolutions during isothermal holdings, or anisothermal cycles.

Thermoelectric power (TEP) measurements have also been used successfully to study carbide precipitation in low carbon steels compared to resistivity [29], or tempering of low carbon martensite [30]. The principles of TEP [31] is to apply to the studied steel specimen a temperature gradient between its two extremities by contact with two pure copper block, and to measure the resulting voltage induced by the Seebeck effect between the two junctions. TEP is sensitive to the crystal defects influencing electron diffusion and phonon propagation, such as atoms in solid solution [32], and is therefore an interesting tool to characterize and quantify precipitation of carbides from oversaturated martensite during thermal ageing.

An original approach to the study of dimensional stability of SAE 52100 has been conducted by NTN–SNR [13,14] using this technique. The aim of the study was to predict the macroscopic dimensional variations as a function of a thermal ageing based on calculations of each contribution through analysis and estimation of each phase transformation kinetics and quantification with TEP. This work comprises two stages:

- Quantification of volume fraction and carbon content of each microstructural constituents through TEP measurements as a function of ageing time and temperature
- Use of these data as input for calculations of dimensional variations of each contribution, and an average calculation to obtain the macroscopic dimensional variation.

TABLE 1 Thermal treatments performed on SAE 52100 [13].

	Martensitic Thermal Treatment		Bainitic Thermal Treatment	
	H	HF	N	NF
Austenitizing	850°C/15 min	850°C/15 min	870°C/15 min	870°C/15 min
Quench/ isothermal holding	Oil	Oil	270°C/20 min	270°C/20 min
Water rinsing	60°C/5 min	60°C/5 min	60°C/5 min	60°C/5 min
Subzero treatment	–	−80°C/1 h		−80°C/1 h
Initial retained austenite content (vol. %)	10.3	4.7	4.7	2.5

From TEP Measurement to Phases Volume Fractions and Carbon Content During Ageing

The study was conducted on samples heat treated according to the cycles of **Table 1** (see also Refs. [13,14,33]). Both martensitic and bainitic heat treatments were studied, and for each treatment, samples were subzero treated to destabilize a part of the retained austenite (F as "freeze" was added to the name of the sample). Different bainitic heat treatments were studied, but only one heat treatment is presented here in details (designed as *N* treatment), because of its academic interest (significant initial amount of retained austenite), even if not completely compatible with bearing applications due to its "low" hardness (57.8 HRC) and "high" initial retained austenite content.

The samples were aged at different temperatures from 110 to 505°C to durations up to 300 h. Ageing was interrupted at logarithmic increasing time steps to measure the TEP evolution for each sample at room temperature.

A schematic of the TEP equipment and conditions used are gathered in **Fig. 1**. The results obtained, expressed as the TEP variation ΔS between initial state (as quenched) and aged at considered time, for the martensitic heat treatment are presented in **Fig. 2** and for the bainitic heat treatments in **Fig. 3**.

For the *martensitic* heat treatments, ΔS increases in two consecutive sigmoidal steps at increasing times and temperatures, identified in **Fig. 2** as A and B. These stages occur sooner when temperature increases, and are assumed to be linked to the same phenomena for all temperatures, based on the time-temperature equivalence presented after. At high temperature and times, ΔS continues to increase linearly, in step C. The first sigmoidal increase, stage A, which is only visible for the ageing at the lower temperatures, is associated to the precipitation of carbon from oversaturated martensite, as metastable ε-carbides. The second sigmoidal increase, stage B, is linked to the precipitation of Fe_3C to the detriment of ε-carbides, from the impoverished martensite. This has been confirmed by TEM observation of samples aged at end of stage A and stage B (respectively, arrows 1 and 2 in **Fig. 2**),

FIG. 1 Schematic of TEP measurement [34].

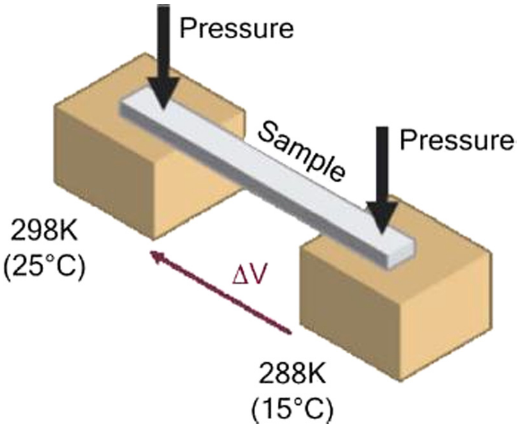

FIG. 2 TEP evolution of the martensitic heat treatment as a function of time at different ageing temperatures, with (HF) and without (H) subzero treatment—H110 stands for H treatment aged at 110°C [13].

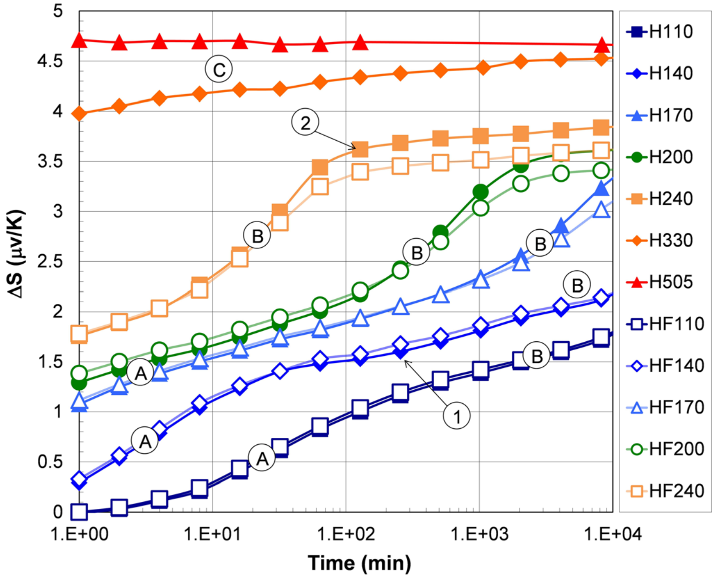

FIG. 3 TEP evolution of the bainitic heat treatment N as a function of time at different ageing temperatures, with (NF) and without (N) subzero treatment—N110 stands for N treatment aged at 110°C [13].

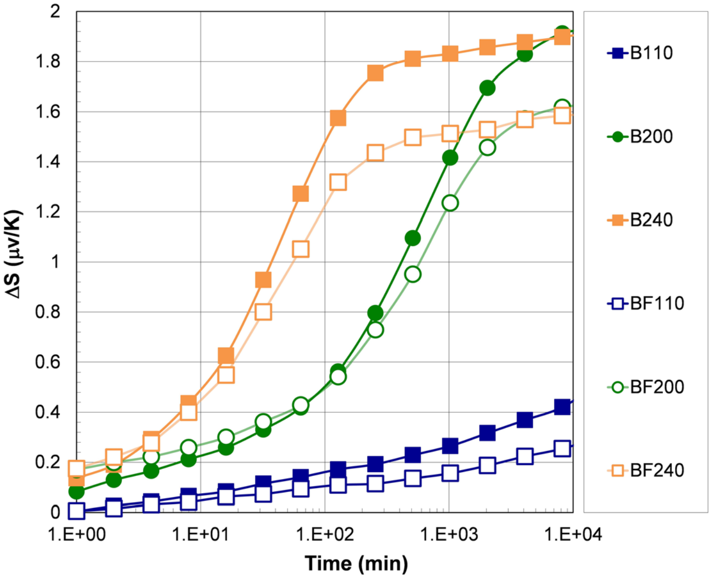

where ε-carbides have been positively identified at the end of stage A by electron diffraction, and Fe_3C at the end of stage B [13,14]. The phenomena occurring during stage C are sustained by TEM observation of H stage aged 40 days at 240°C (see Fig. 5.14 to 5.16 of Ref. [13]).

While subzero treated HF samples present during stage A ΔS with the exact same amplitude to H samples, during stage B, the curves for HF samples are no longer identical, but present slightly lower ΔS. The only difference between the two treatments being their initial retained austenite content (10.3 vol. % for H, and 4.7 vol. % for HF), this difference is assumed to be linked to the decomposition of retained austenite that seems to occur simultaneously to the precipitation of Fe_3C carbides.

Stage C is assumed to be caused by the phenomena occurring during fourth stage of tempering: recovery of the dislocation structure, recrystallization, and the coarsening of carbides (see the section "From Metallurgical Phenomena to Dimensional Variations"), later referred to as recovery.

For the *bainitic* heat treatment N (**Fig. 3**), ΔS increases in only one sigmoidal stage, with a difference between subzero treated NF and non-treated N samples, equivalent to the observation mentioned earlier for martensitic samples. This sigmoidal increase is attributed to the transformation of nanometric Fe_3C carbides

FIG. 4 Dark field TEM image of N bainitic heat treatment in its initial state, showing two carbide populations: elongated large carbides, and nodular nanometric carbides—produced with indicated diffraction reflexions (from Ref. [13]).

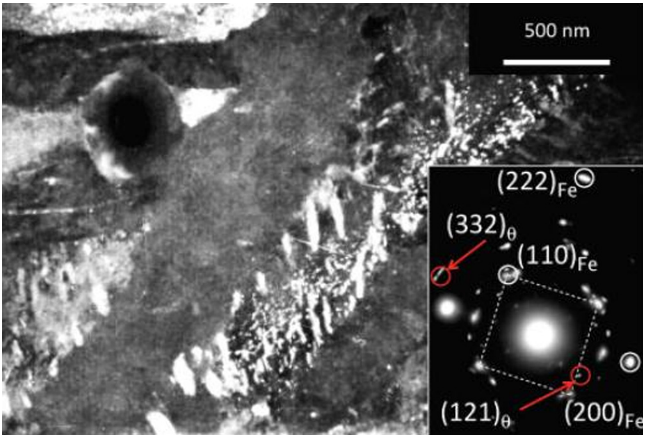

present in the initial microstructure (**Fig. 4**) into larger Fe_3C carbides (see Fig. 5.22 and 5.23 of Ref. [13]). Measurements were also made for the other bainitic heat treatments, with and without subzero treatment, and present the same behavior than that of N.

As increasing temperature seems to shift the curves towards shorter times, and as it has been done frequently in the literature, the results were treated with a time-temperature equivalence according to an Arrhenius law [14], to transfer measurements of all times and temperatures to equivalent times at 110°C, the lower ageing temperature investigated.

For *martensitic* heat treatments (**Fig. 5**), this time-temperature equivalence lead to the two following different activation energies corresponding to the best fit shown in **Fig. 5**: 120 kJ/mol for the low temperature ageing from 110 to 240°C, and 190 kJ/mol for higher temperature ageing (330 and 505°C). The activation energy for the low temperature range, 120 kJ/mol is close to that of carbide precipitation during tempering of martensite [21]. The activation energy for the high temperature range is close to that for recovery in α-iron [14].

An equivalent approach was used in Ref. [13] to estimate the activation energy for the retained austenite decomposition, assuming that the difference between H and HF ΔS is only connected to retained austenite decomposition. ΔS differences between H and HF were normalized to the maximum difference at higher times (identical for all ageing temperatures), and an Arrhenius law was applied with an activation energy of 125 kJ/mol, very close to that obtained for carbide precipitation in the previous paragraph. This value confirms results obtained previously in

FIG. 5 Experimental (dots) and modeled (curves) TEP evolution for martensitic heat treatment H: macroscopic TEP evolution (ΔS_H) and individual contributions to TEP evolution (ΔS_ε, ΔS_θ, $\Delta S\gamma_R$, ΔS_R) as a function of equivalent time at 110°C—H110 stands for H treatment aged at 110°C [13,14].

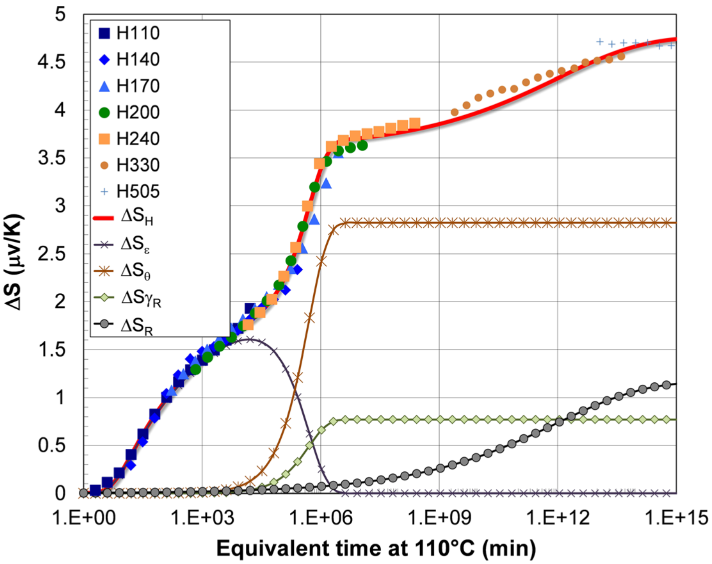

NTN–SNR on retained austenite content measured by X-Ray diffraction as a function of ageing times and temperatures, and other works published on SAE 52100 [6,35].

For *bainitic* treatment (**Fig. 6**), a lower activation energy of 80 kJ/mol was obtained using the time-temperature equivalence leading to the best fit shown in **Fig. 6**.

This approach is assumed because it is believed in this study that carbon diffusion controls the kinetics of precipitation.

These master curves (**Figs. 5** and **6**) were then used to estimate the *evolution of volume fraction and carbon content* of the different constituents of the microstructure, through their individual contribution to TEP evolution.

The following assumptions were made [14]:

- Retained austenite decomposition and cementite precipitation are simultaneous, as the same activation energies and experimental results seem to show.
- Some carbon is segregated on dislocations in the initial state, in particular because of the water rinsing at 60°C before ageing. This segregated carbon is more stable than in ε-carbides, but even more stable within Fe_3C. That means that the initial carbon segregated on dislocations will not participate to the formation of ε-carbides, but will to the formation of Fe_3C.

FIG. 6 Experimental (dots) and modeled (curves) TEP evolution for bainitic heat treatment N: macroscopic TEP evolution (ΔS_N) and individual contributions to TEP evolution(ΔS_θ, $\Delta S\gamma_R$, ΔS_R) as a function of equivalent time at 110°C [13,33].

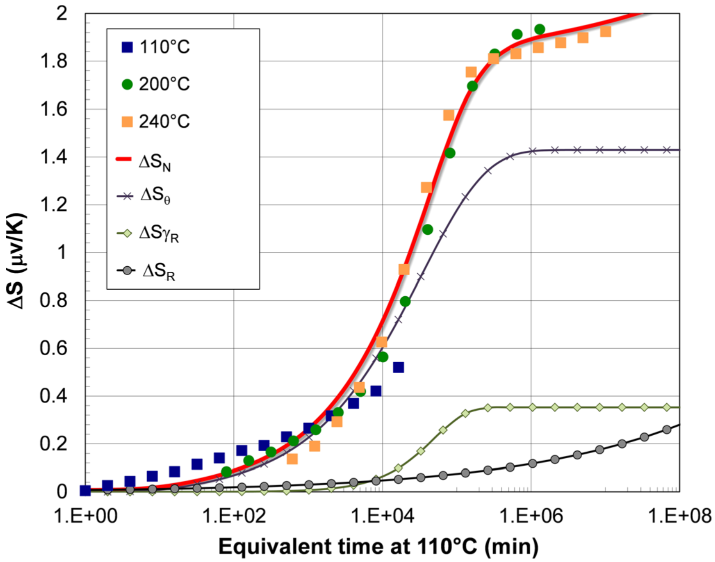

- Undissolved carbides are assumed not to evolve during the ageing times and temperatures involved in this study, and are therefore neglected hereafter.

The scenario for the evolution of TEP is the following (considering an initial microstructure as described in Appendix A) [14]:

- Stage A: ε-carbides are precipitated from the carbon rejected from the oversaturated martensite.
- Stage B: Fe_3C carbides precipitate using the carbon segregated on dislocations, the carbon remaining in solid solution in martensite, and released from the decomposition of ε-carbides that dissolve because they are less stable than Fe_3C. Simultaneously, retained austenite decomposes into a mix of ferrite and cementite.
- Stage C: Recovery of dislocation structure and coarsening of martensite laths occur.

Based on these assumptions and scenario, an analytical approach was built, using Johnson–Mehl–Avrami–Kolmogorov [14] (JMAK) empirical formulae for the kinetics of the precipitation of ε-carbides and Fe_3C, and for the recovery of dislocations and lath coarsening (Appendix A).

The macroscopic TEP is considered to be the volume average of the two individual contributions to TEP of the martensitic phase (the variation of carbon in solid solution in the martensite and the recovery), and of the retained austenite

(Appendix A). The TEP master curves of H and HF heat treatments as a function of equivalent time at 110°C were then used to adjust a number of parameters while others were measured or gathered from publications (Appendix A) [14]. The interpolated parameters were all confronted to values available in the literature and found to be in agreement with them [14]; in addition, the interpolated TEP curves fit quite well with the experimental data (**Fig. 5**).

The same analytical approach was conducted on the *bainitic* heat treatments [13,33], taking into consideration three main microstructural evolutions modelled by JMAK laws similar to martensitic heat treatments:

- Transformation of nanometric carbides into larger carbides
- Simultaneous retained austenite decomposition
- Recovery

The approach, similar to that used for martensitic structures, and its parameters are described in Appendix A. Again, the interpolated curve compared to the experimental data fit rather well (**Fig. 6**).

From Phase Volume Fractions and Carbon Content to Macroscopic Dimensional Variations

The macroscopic dimensional variations can be calculated from the individual contributions of each phase, as far as the microstructure of SAE 52100 can be understood as a composite material (see Refs. [13,14,33]). This can be achieved either through the use of simple models, like in Ref. [14], where the minimal and maximal value of dimensional variations were estimated by averaging the stresses (uniform strain, Voigt) or the strains (uniform stress, Reuss) in the volume, either with more complex approaches such as self-consistent model or Ponte Castaneda-Willis (also called homogenization techniques) used in Ref. [13], that take into account the morphology and relative layout of the phases, and their mechanical interactions. Anyhow, these last models are more precise, but also more complicated to use. It is therefore chosen in this publication to use the Voigt and Reuss estimations that already give relatively precise assessment of the macroscopic variations.

Literal expressions used for the calculations of volume fractions and eigenstrains can be found in Appendix A.

For a given time and temperature, it was then possible to estimate the macroscopic dimensional variation limits (Voigt, Reuss). Carbon concentrations in the different phases and the fraction of decomposed retained austenite are the main input parameter of this model. The experimental measurements are in good agreement with the estimations (**Fig. 7**) [13,14].

As an example of use, the estimation of dimensional variations for equivalent time at 110°C is represented in **Fig. 8** for H and HF martensitic heat treatments, with two different initial retained austenite content [13,14]. It is possible to compare the influence of retained austenite content for similar austenitizing temperature and quench.

For *bainitic* heat treatment, a similar model was developed [13,33].

FIG. 7 Experimental (dots) and modeled (curves) dimensional variations of martensitic H heat treatment at experimental temperatures [13,14].

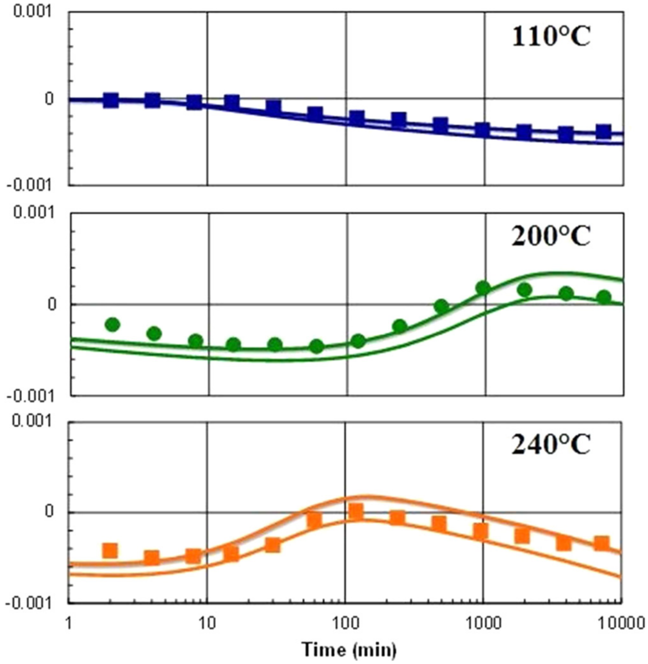

It is assumed that only decomposition of retained austenite and recovery are the causes of dimensional variations (see Appendix A). The results of the model and individual contributions for equivalent times at 110°C, and the comparison of experimental data and model at experimental times and temperatures are gathered, respectively, in **Figs. 9** and **10** [33].

DISCUSSION ON RELATIVE INFLUENCE OF INDIVIDUAL CONTRIBUTIONS TO DIMENSIONAL VARIATIONS

In industrial practice, hardened bearing steels are never used as quenched, but tempered, in order to reduce the inherent brittleness of high carbon steels.

Selection of Tempering

Tempering after quenching is the beginning of the ageing process described in the section "From Metallurgical Phenomena to Dimensional Variations" and characterized in the section "From the Evaluation of Individual Contributions of Each Phenomenon to the Prediction of Macroscopic Dimensional Variations," and will be more or less advanced depending on the tempering conditions. Depending on the extent of the tempering, i.e., temperature and duration, stage A and possibly stage B

FIG. 8 Estimated macroscopic dimensional variations (Voigt, Reuss) and individual contributions of phases to macroscopic dimensional variations (ε, θ, α', γ_R) for equivalent times at 110°C. (*a*) H martensitic treatment with 10.7 vol. % retained austenite, (*b*) HF martensitic heat treatment with 4.7 vol. % retained austenite [14].

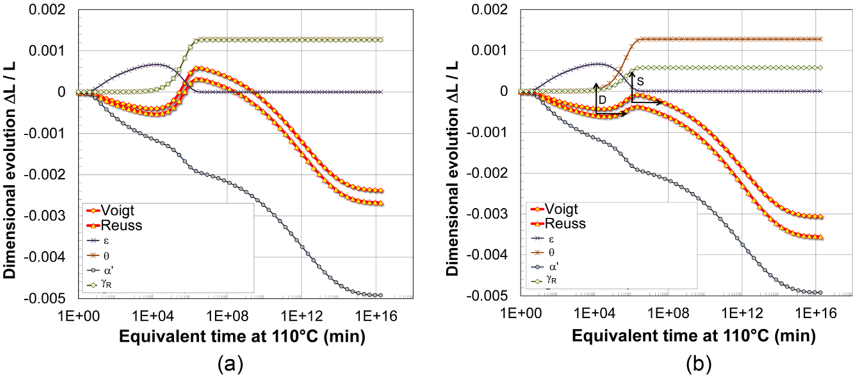

(a) (b)

FIG. 9 Macroscopic dimensional variations estimation (Voigt, Reuss) for N bainitic heat treatment for equivalent times at 110°C, and individual contributions (α, γ_R) [33].

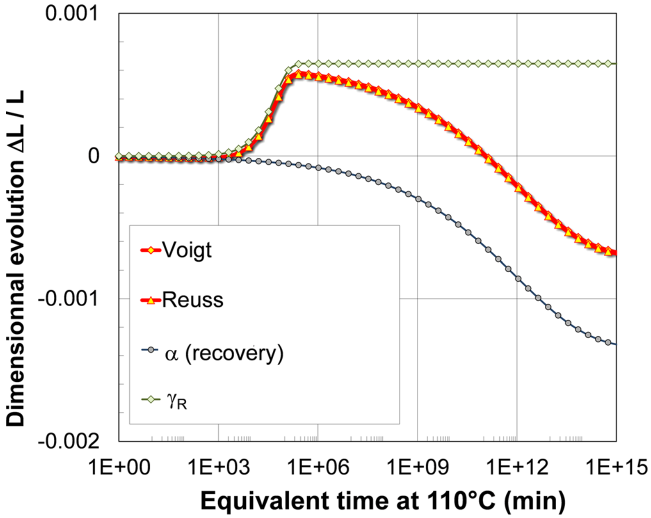

FIG. 10 Experimental dimensional variations (dots) and Voigt and Reuss (superimposed curves) limits for bainitic heat treatments with different initial retained austenite contents (N treatment = 4.7 vol. % of retained austenite) for an ageing at 200°C [13,33].

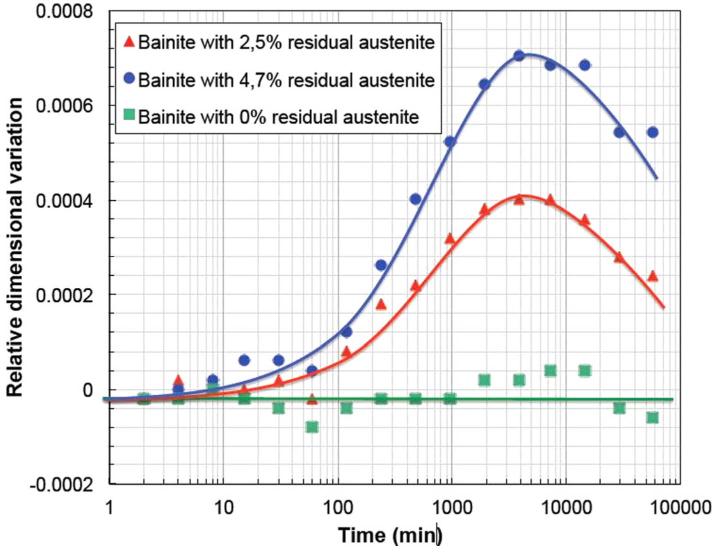

described in the section "From the Evaluation of Individual Contributions of Each Phenomenon to the Prediction of Macroscopic Dimensional Variations" occur during tempering.

In service, the material will undergo an additional thermal ageing, similar to tempering, during which the phase transformations initiated during tempering continue.

Depending on tempering conditions, the component will present an expansion in service if only stage A occurred during tempering or a contraction if stages A and B (total decomposition of retained austenite) occurred. It is to be reminded that dimensional evolutions can occur even at low temperatures given that enough time has passed.

Finally, in the case of SAE 52100, depending on the application, different temperings are applied, resulting in different properties and advantages/shortcomings:

- "Low temperature" or standard tempering (only stage A occurs during tempering)—D treatment: the hardness obtained is high for good RCF performance and no dimensional stability is guaranteed.
- "Higher temperature" tempering (stages A and B occur during tempering)—S treatment: the hardness obtained is lower than that of D tempering, but dimensional stability is guaranteed, as no expansion due to retained austenite

decomposition will occur, but contraction at long operating times, or high temperatures, or combinations thereof. These temperings are used for bearings subjected to higher temperatures.

The actual temperatures/times of D and S temperings as they are practiced at NTN–SNR were used to calculate the equivalent times of ageing at 110°C for a SAE 52100 steel, so that the as-tempered state for D and S are reported in Fig. 8.

Relative Contributions of Phases During Ageing

In Fig. 8, the relative contributions of each phase to macroscopic dimensional variations are reported, so that is now possible to quantify the phenomena described in the section "From Metallurgical Phenomena to Dimensional Variations" and their dependence on influence parameters.

- Precipitation from martensite
    - ○ Contraction of martensite and recovery: it is the only contraction contribution, but has the largest amplitude. It is a cubic function of carbon content, and therefore highly dependent on the initial carbon content of the martensite. For higher times and temperatures, recovery is responsible for the contraction.
    - ○ Precipitation of ε-carbides: the contribution is positive creating an expansion only proportional to the carbon used to form the carbides; therefore closely linked to the contraction of the martensite that releases carbon.
    - ○ Precipitation of Fe_3C: the contribution is also positive, creating an expansion that slows down even more the global contraction of the overall contribution of martensitic fraction. This expansion is proportional to the carbon content used to create these carbides, i.e., released by martensite, but also carbon available elsewhere in the microstructure such as that segregated on dislocations, according to the model presented in the section "From the Evaluation of Individual Contributions of Each Phenomenon to the Prediction of Macroscopic Dimensional Variations". In the cases presented in Fig. 8, the size increase associated to cementite precipitation is of the same order of magnitude (case of H heat treatment, as curves for both contributions are superimposed on the graph of Fig. 8(*a*)), or even higher than the expansion produced by retained austenite decomposition (case of HF heat treatment, on the graph of Fig. 8(*b*)).
- Decomposition of retained austenite: it produces an expansion all the more important that the initial retained austenite content is high and that it contains a lower carbon concentration (eigeinstrain as a function of carbon content of retained austenite is a decreasing function).

The increase of initial carbon concentration in solid solution in martensite will not dramatically change the balance of the phenomena, since it will increase the contraction linked to martensite, but also the expansion resulting from carbide precipitations. The effect of carbon segregated on defects will be more influential since it only influences the expansion during Fe_3C precipitation.

Bainitic/Martensitic Heat Treatments

In the case of bainitic heat treatments, the only phenomenon is the decomposition of retained austenite. This expansion is not compensated by the overall contraction of the martensitic phase because these stages have already occurred during the isothermal bainitic transformation.

Therefore, if there is a given amount of retained austenite in the initial microstructure—that could be the case since bainitic heat treatments on bearing steels are generally realized close to M_S to keep a hardness compatible with bearing applications, but as a consequence require a long holding time to complete austenite transformation—the expansion in service will be more important that in the case of martensitic heat treatments for equivalent retained austenite content. For example, the maximal dimensional variation in service in case of H martensitic heat treatment with a subsequent D tempering (standard tempering) is estimated to 9×10^{-4}, corresponding to a size change of 8.7×10^{-5} for each % of decomposed retained austenite, against a size change of 7×10^{-4} for N bainitic heat treatment (4.7 vol. % retained austenite) or 4×10^{-4} for the bainite with an initial retained austenite content of 2.5 vol. % corresponding to approximately 1.5×10^{-5} per % of decomposed retained austenite in the case of bainitic heat treatment.

As a conclusion, bainitic heat treatments can be considered for bearing steels for many reasons such as toughness increase; however, it will be necessary to adapt the heat treatment to remove completely untransformed austenite, not to produce in service dimensional variations detrimental to bearing performance.

Advantages of Retained Austenite: Performance Increase Under Severe Conditions

DECOMPOSITION OF RETAINED AUSTENITE UNDER MECHANICAL LOADING

Martensitic transformation of austenite is a diffusionless mechanism that is triggered when a sufficient driving force is reached [24]. This driving force is generally a large undercooling below M_S (classical quench hardening), but as martensitic transformation goes along with deformation, an external applied stress can complement or replace the chemical driving force and produce martensitic transformation. Therefore, under stress or strain, retained austenite can be transformed into martensite, creating a local expansion inducing compressive residual stresses.

As retained austenite is soft, it is the first constituent of the microstructure to be subjected to plastic strain.

This fact is illustrated by the compression strain hardening curves of SAE 52100 or similar bearing steel (100Cr6mod according to Ref. [36], presented in more detail in the next section) holding different initial retained austenite contents gathered in **Fig. 11**. These results were obtained from static compression tests with successive increasing stress steps followed by unloading, by plotting the plastic strain measured after unloading, as a function of stress. Microyield strength of SAE

FIG. 11 Compression strain-hardening curves for 100Cr6 steel with D (8 vol. % of retained austenite) and S (< 3 vol. % of retained austenite) tempering, and of 100Cr6Mod (18 vol. % of retained austenite) [46].

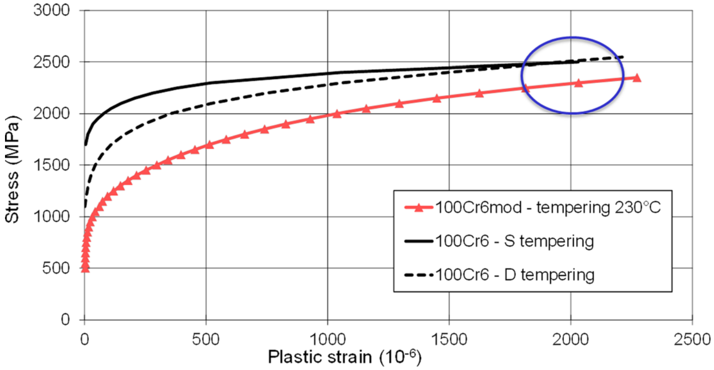

52100 and similar steels is all the more low that its retained austenite content is high: the 18 vol. % retained austenite containing steel yields at stresses a third of that of stabilized SAE 52100 steel containing no retained austenite. However, it must be noticed from **Fig. 11**, that retained austenite has a high strain hardening ability, so that the three different combinations of steel and heat treatment present similar levels of conventional yield strength at 0.2 % (2000×10^{-6}). Similar results were discussed in Ref. [37].

This property of retained austenite to destabilize at relatively low stresses has practical consequences.

In RCF, the subsurface material subjected to shear stresses presents such a decomposition of retained austenite. This was documented by Voskamp [38].

But mostly, this property gives to stable retained austenite containing steels significant enhancements of some mechanical properties [24]:

- Increase of toughness [39] because a network of retained austenite region breaks the continuity of brittle phases, and complicate crack propagation, through crack branching, crack blunting, and transformation induced plasticity that reduce stress concentration.
- Structural fatigue, depending on the conditions [40,41].
- Rolling contact fatigue resistance, especially under severe conditions such as contaminated or deficient lubrication [15–18].

Rolling Contact Fatigue Performance Enhancement Under Severe Conditions

Today, thanks to steelmaking improvement, bearings fail less and less from inclusion induced subsurface rolling contact fatigue, but from other failure mechanisms linked to severe operating conditions. Among these, deficient and contaminated lubrication produce surface initiated failures, that have been extensively studied, and material solutions have been designed to meet these more stringent requirements.

Studies describing the major factors influencing contaminated lubrication failures are summarized in Ref. [19], and the damage process with the relevant material properties are described in Refs. [19,20]. Hard particles are carried by the lubricant into the contact, and damage the surface by indenting it. The dents present a detrimental topography: holes with raised ridges due to the material's plasticity, that produce by over-rolling overpressures leading to crack initiation in the vicinity of the dent, inducing in the end a typical V-shaped spalling. Either the size of the dents, the height of the raised ridge, the slope of the dent or the ratio r/c (r = radius of the raised ridge, c = half value of the dent width) have been mentioned to be the more prevalent parameters on the nocivity of these dents [19,42].

To delay crack initiation, material properties should lead to the reduction of the dents harmfulness, through a reduction of the above mentioned geometrical characteristics: a high hardness and a good intrinsic ductility are answers to these requirements. Then, to slow down propagation of the microcracks, a good toughness is an attractive feature. Retention of stable retained austenite, providing ductility and toughness to the surface combined with a high hardness is the usual solution for these applications [15–18].

Two categories of solutions have been developed over years to answer this difficult challenge [43] and are still under optimization:

- Through-hardening materials with special alloying to promote stable retained austenite [20,36,44–46]
- Case-hardening (carburizing [17,47,48] or carbonitriding [17,18,20,44]) of specific carburizing steel grades, or of SAE 52100 [49,50].

In the following, two material solutions, one of each category, are presented and compared to standard SAE 52100 (**Table 2**).

Modified SAE 52100 (also referred to as 100Cr6mod) has been designed from SAE 52100, that in itself cannot produce a retained austenite with the appropriate

TABLE 2 Materials characteristics of damage tolerant materials solutions compared to standard solution.

	Modified SAE 52100	Carbonitrided 100Cr6	Standard SAE 52100 (D)
Surface hardness	60–63 HRC	65–67 HRC	61–63 HRC
Core hardness	60–63 HRC	63–65 HRC	61–63 HRC
Surface retained austenite content	15–20 vol. %	15–20 vol. %	6–12 vol. %
Core retained austenite content	15–20 vol. %	8–10 vol. %	6–12 vol. %
Residual stresses	–	−200 MPa	–

FIG. 12 Indent geometry for damage tolerant materials solutions for a 200 μm radius tip Rockwell indentor: (*a*) ridge height as a function of indentation load and (*b*) slope (D/p) as a function of indentation load where D is the dent diameter, and p, its depth.

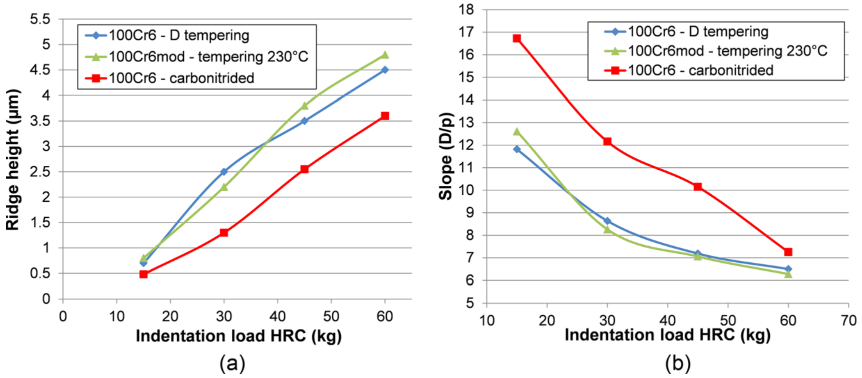

(a)

(b)

content and stability, by adding Manganese to retain austenite after hardening, and Silicon to stabilize it [36,46] (see effects of alloying additions in the section "Promoting Retained Austenite by Alloying)".

SAE 52100 carbonitriding promotes the retention of retained austenite in the surface through the action of nitrogen and carbon. The formation of nitrides and carbonitrides gives to the surface a hardness unrivaled by any standard through-hardening heat treatment of the same steel (Table 2).

The indentation resistance of the materials is characterized through the measurement of the topography of the dents induced by loading a Rockwell indenter on the surface of steel samples. Some typical features, the dent diameter to depth ratio (ratio of the diameter of the dent to its depth) and ridge height, are reported as a function of indentation load for a tip of 200 μm radius in Fig. 12. A high value of diameter to depth traduces a less severe dent, and a lower stress concentration (same evolution as r/c).

100Cr6mod, despite its high retained austenite content, presents a dent topography similar to that of standard SAE 52100, whereas carbonitrided SAE 52100 presents less severe dents, according to its higher hardness and retained austenite content (Fig. 12). It seems that hardness is the controlling factor on harmfulness of the indents.

Contaminated lubrication tests on ball bearings were realized with many different carbonitriding cycles to optimize the process in terms of retained austenite content and hardness, according to the procedure described in Ref. [19]: initial contamination step with M50 powder, and then endurance in clean lubrication conditions under 2.8 GPa. From the results gathered in Fig. 13, it can be concluded

FIG. 13 Influence of retained austenite content and hardness on RCF performance under contaminated lubrication: (*a*) influence of retained austenite content on L10 life for carbonitrided 100Cr6 classified into hardness ranges (775–810 HV, 860–900 HV); (*b*) influence of hardness on L10 life for carbonitrided 100Cr6 classified into retained austenite content ranges (7–8 vol. %, 17–23 vol. %, 26–31 vol. %).

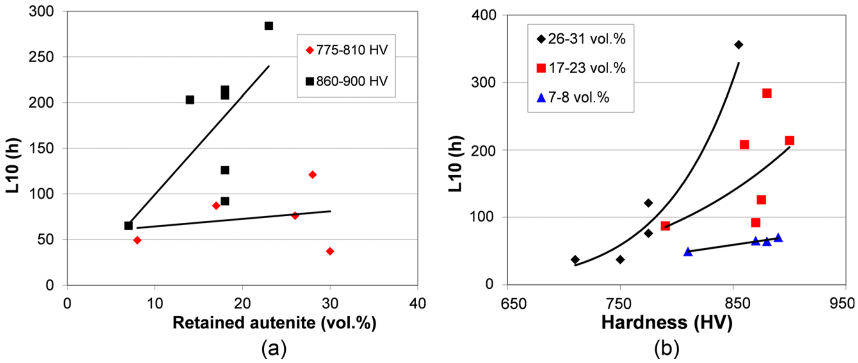

that both a high hardness and a high retained austenite content are necessary for efficiently increasing contaminated lubrication RCF performance.

The two proposed solutions are then compared in terms of clean and contaminated lubrication rolling contact performance (Fig. 14) with the standard solution through-hardened SAE 52100 with D tempering, as the use of this tempering leads to a higher hardness and a higher content of retained austenite compared to S

FIG. 14 RCF performance under clean and contaminated lubrication of damage tolerant materials solution.

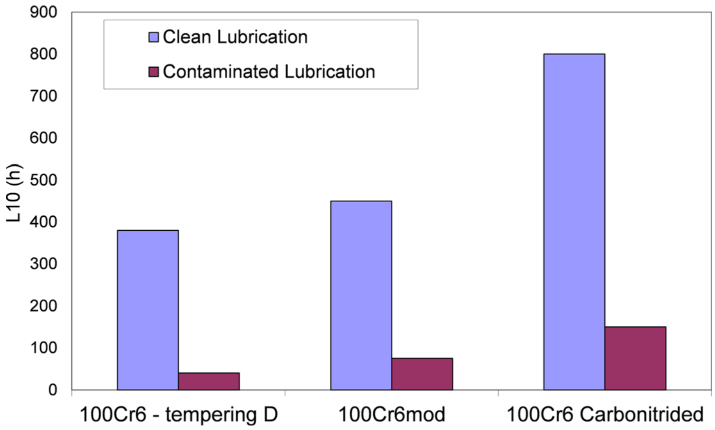

tempering, and will therefore perform better under contaminated lubrication. 100Cr6mod only brings a relative improvement to contaminated lubrication performance of standard SAE 52100, compared to the potentiality of carbonitrided SAE 52100. The very good performance of carbonitrided SAE 52100 can be explained by a much better resistance to indentation that provides the surface with dents that are less nocive, delaying crack initiation. These results suggest that both retained austenite intrinsic plasticity and compressive residual stresses inherent to the carbonitriding process impede the propagation of cracks formed in the vicinity of the dents, and that in the case of 100Cr6mod, subjected to dents as nocive as that of standard SAE 52100, initiation of cracks and their propagation are only slightly hindered by the ductility of retained austenite.

Retained Austenite Control

STABILITY AND STABILIZATION OF RETAINED AUSTENITE

Complex mechanisms govern the stabilization and stability of retained austenite, complicating a clear understanding of the phenomena and the relative influence of the implicated parameters (steel composition, heat treatment, service conditions,…) on the stability/stabilization of retained austenite.

Definitions of stability and stabilization must first be settled and the difference between the two terms clarified. Stability is the property of the retained austenite to resist transformation under thermal or mechanical conditions. Stabilization corresponds to the phenomena or mechanisms responsible for the retention of austenite in conditions where it should be no more present. Stabilization of retained austenite originates from three different sources [3,39].

Chemical stabilization of austenite is produced by the action of alloying elements on the equilibrium temperature and transformation kinetics of steel microstructural constituents [3,39]. Enrichment of austenite in fcc-stabilizer elements lowers the M_S temperature of austenite, stabilizing it towards martensitic transformation. These elements are in the order of stabilization efficiency C, Mn, Cr, Ni, and Mo. This effect can be obtained by specific alloying of the steel, or heat treatment conditions enabling diffusion and promoting partitioning of these elements, especially carbon, into austenite. This is, for example, the case for very low cooling rates, or isothermal holding at temperatures high enough to enable carbon diffusion from martensite to the surrounding austenite. This partition of carbon in austenite promotes the retention of retained austenite at room temperature after quenching.

Thermal stabilization [39,51] corresponds to the segregation of interstitial atoms (C, N) to dislocations to form atmospheres that inhibit dislocation mobility. These dislocations are located either at the γ/α' interface, and impede movement of this interface, stopping further martensitic transformation because formation of new martensite nuclei requires creation and movement of dislocation at γ/α' interface, or in the phases themselves impeding stress relaxation. Such segregation is favored by low cooling rates, by isothermal holding, or by interrupted quenching (marquenching).

Mechanical stabilization is connected to the influence of stress field on martensitic transformation. Martensitic transformation can be induced by favorable elastic or plastic strains in austenite (nucleation on pre-existing dislocations). Any relaxation of elastic stresses in austenite by tempering or interrupted quench, or dislocation rearrangement, can hinder further transformation.

On the other hand, small volumes of retained austenite can be stabilized because of the high hydrostatic pressures from transformed neighboring martensite, or because surrounding areas cannot accommodate the strains and stresses resulting from martensitic formation [52]. This is probably the source of stability of very small retained austenite regions or interlath retained austenite, or in case of grain refinement.

Stability of retained austenite depends on the type of loading

Thermal stability qualifies the resistance of austenite to transformation under thermal conditions. Two types of thermal stability can be defined: thermal stability to a further quenching/cooling, or thermal stability to thermal ageing.

Under further quenching or cooling, retained austenite transforms to martensite, and all the stabilization mechanisms described previously that hinder martensitic transformation will increase thermal stability to quenching. This type of thermal stability has been widely discussed in the literature, particularly in relation to subzero treatment that enables transformation of a larger amount of retained austenite, that will be discussed in the next section [5,6,51].

Under thermal ageing, diffusion is possible, and retained austenite decomposes into a mix of ferrite and carbides, sometimes referred to as bainitic [24]. Some say that retained austenite decomposition occurs in a similar way as that of fresh austenite of identical composition would according to TTT curves [53]. In these terms, thermal stability to thermal ageing is retained austenite's ability not to decompose during service under thermal ageing. In other words, this retained austenite thermal instability in service leads to the dimensional variations discussed in the second section of the paper.

Mechanisms that increase thermal stability to quenching, such as carbon partitioning into austenite (chemical stabilization) or carbon segregation to dislocations at γ/α' interface (thermal stabilization), can tend to decrease thermal stability under thermal ageing. A higher carbon concentration in retained austenite provides a higher driving force for its decomposition in ferrite and carbides, and a higher dislocation density in retained austenite will favor heterogeneous nucleation of carbides.

It is therefore important to bear in mind the difference between thermal stability to quenching and linked mechanisms that will promote retention of retained austenite after quenching, and thermal stability to thermal ageing that can in some cases be subjected to the contrary effects for the same mechanisms.

Mechanical stability is the ability of retained austenite to resist transformation under mechanical stresses or strains. Under mechanical stresses, retained austenite decomposes into martensite.

Retained austenite of low mechanical stability will transform in martensite under load; this phenomenon is called the transformation induced plasticity effect (TRIP) and is used for TRIP steels [54], for example for automotive sheet steels that can undergo high strains (formability) combined with a very high energy absorption ability (use in safety components).

Retained austenite of high mechanical stability is strengthened by strain hardening without transforming.

PROMOTING OR SUPPRESSING RETAINED AUSTENITE BY HEAT TREATMENT

Heat Treatment Parameter Influence on Retained Austenite

Many studies have been carried out on the influence of heat treatment conditions of classical bearing steel on the amount of retained austenite [4–9], and its thermal stability, through its practical consequences on dimensional stability.

Pearson [4], in his state of the art on size change for bearing steels, underlined the parameters influencing retained austenite content and its dimensional consequence for SAE 52100 after standard heat treatments: alloy composition, austenitizing cycle (time and temperature), quenching rate, and tempering conditions. For a variability of industrial heat treatment conditions and facilities, he estimated the dispersion of size change that can be found for standard treated SAE 52100: for an ageing of 3000 h at 150°C, the size expansion can vary from 7×10^{-4} to 11×10^{-4}, illustrating the influence of the different heat treatment conditions used depending on the bearing manufacturer and facilities.

It is necessary to be reminded that the main objective of the standard heat treatment, as was discussed in the "Discussion on Relative Influence of Individual Contributions to Dimensional Variations" section, is the achievement of a good RCF resistance, and therefore a high hardness for applications that do not need stabilizing heat treatments, and not necessarily require a minimum size change. It is also important to underline that heat treatment solutions can be chosen out of hardness and dimensional stability considerations, for example to minimize distortions or avoid quench cracking, and that many criteria are accounted for to design the heat treatment.

In the 1970s, Franklin [8] conducted an extensive study on the effect of all these parameters on retained austenite content (without measuring its consequent dimensional size change). The main conclusions also obtained by other authors [53,55] are summarized in the following.

Influence of Austenitizing Temperature and Time. When the austenitizing holding time and the temperature increase, more carbides are dissolved and more carbon and alloying elements are present in solid solution in austenite. As a consequence, M_S temperature lowers, and more austenite is retained after quenching (chemical stabilization).

Influence of Quenching Rate. Quenching rate depends on the quenchant medium used. A quicker cooling rate produces lower retained austenite contents. Untransformed austenite is stabilized (thermal stabilization) by a slower cooling rate, by enabling the diffusion of carbon atoms to defects lowering the potential for martensite formation, and therefore increasing the subsequent retained austenite content.

Influence of Interrupted Quenching. Martempering or marquenching consists in interrupting the quenching at temperatures just below M_S. It is commonly used for 100Cr6 bearing steel, in order to reduce heat treatment distortions and quench cracking likelihood. Untransformed austenite is stabilized by this isothermal holding, to a greater extent with increasing time and temperature. It is believed that this is linked to auto-tempering of newly transformed martensite relaxing stressed regions; thus reducing potential for martensite nucleation (mechanical stabilization).

Influence of Quenching Temperature. Yajima [15] correlated quenching temperature for a SAE 52100 steel quenched from 840°C into oil, and tempered at 160°C for 1 h, with its retained austenite content. He showed that the curve is dome shaped, and present a maximum of 8 vol. % of retained austenite for a quenching temperature of 55°C, and that the retained austenite content is reduced for lower (6 vol. % for 13°C) or higher (5 vol. % for 140°C) quenching temperatures. Luty [9] showed that decreasing quenching temperature between 80 and 15°C reduces retained austenite content and consequent dimensional variations.

Influence of Tempering Time and Temperature

Higher temperature and times will lead to lower retained austenite content. For a SAE 52100 steel, temperatures lower than 200°C will not lead to significant lowering of retained austenite content [4,5].

According to Ref. [53], a work from the 1970s, it is possible to estimate quite precisely the precise amount of retained austenite to be expected depending only on M_S temperature (influence of austenitizing time and temperature) and on the time spent between 700 and 300°C (Δt_{300}^{700}) during cooling (influence of quenching rate):

$$\gamma = \exp[-0.011(M_S - 20)(1 - \mu)]$$
$$\text{with } \mu = 0.41[1 - \exp(-0.03(\Delta t_{300}^{700})^{0.6})]$$

This formula takes into account the influence of cooling rate on the formation of intermediary constituents as pearlite or bainite, through an estimation of subsequent M_S and remaining amount of austenite still to be transformed after this intermediate phase transformation. Unfortunately, it cannot take into account intermediate quench interruption such as marquench heat treatments that present an isothermal holding below M_S before final quench, whereas it is known that it increases the amount of retained austenite.

Intentional Removal of Retained Austenite

Different methods have been tried to reduce retained austenite content over the years.

Subzero treatment consists in an additional subzero quenching after the standard quenching to room temperature. Many studies were realized in order to optimize temperature and durations of this treatment. Theoretically, decreasing temperature below M_F, which is below room temperature for bearing steels, is enough to complete the transformation. Experience shows that it is not necessary to cool below an optimal temperature, and that the components need to remain for a certain duration at this temperature to transform a maximum of retained austenite [5,10,55]. For SAE 52100 steel, a good compromise is the use of a temperature of −70°C [56]. The studies also showed that it is impossible to destabilize the total amount of retained austenite, and that a small amount always remain after subzero treatment.

Studies also showed that subzero treatment should be performed without delay after quench [5,10,55]. A holding at room temperature is enough to stabilize a part of the retained austenite (by segregation of carbon to dislocations and γ/α' interface–thermal stabilization). This stabilization can be quantified by the amount of undercooling necessary to restart martensitic transformation. It is even more important that the temperature is high, that the duration of isothermal holding is long, or that the amount of martensitic transformation is large.

Water rinsing consists in submitting the components to a soaking in a water tank at 15°C–20°C, after oil quench usually realized between 40 and 60°C. It has been shown that this step reduces a portion of the retained austenite, and consequent dimensional variations: it is possible to reduce the expansion by 40 % [6,9].

As subzero treatment can only partially transform retained austenite, *tempering* (stabilizing heat treatment) is to date the most effective way to suppress retained austenite. For SAE 52100 and other low alloyed steels, tempering temperature must be selected in excess of 200°C for a significant reduction of retained austenite content, and at least 230°C for efficient removal of retained austenite [4]. At tempering temperatures below 200°C, as it was discussed previously, tempering has a stabilizing effect on retained austenite [4,5,10].

In the case of special high-alloy steel [5,53,55] (or high temperature steels), tempering between 500 and 600°C leads to precipitation of carbides from austenite during isothermal holding, reducing local carbon content, and increasing M_S, so that when the material is quenched after tempering, fresh martensite (or secondary martensite) is formed. These steels must be subjected to multiple temperings in order to destabilize more retained austenite after tempering, and temper this fresh martensite. To obtain isothermal decomposition of retained austenite during temperature, as for low alloyed steel, tempering should be realized at temperatures above 700°C.

Intentional Stabilization of Retained Austenite

Different attempts were made to stabilize retained austenite through heat treatment: for example, controlled and slowed down cooling around M_S and below [16], complete dissolution of carbides during austenitizing and double isothermal holding: the first below M_S, and the second above M_S [57] (this heat treatment is also called martempering). Bainitic heat treatments were also considered [58], but have already been discussed in the section Discussion on Relative Influence of Individual Contributions to Dimensional Variations.

Some experiments were also realized in NTN–SNR as to the possibility of stabilizing retained austenite in different through-hardening steels, but none were as efficient as alloying.

PROMOTING RETAINED AUSTENITE BY ALLOYING

C is the element that has the strongest lowering effect on M_S for retention of austenite after heat treatment, and the most used for the control of retained austenite, but this is realized through the design of the heat treatment, and has already been discussed in the previous section. An increase of carbon stabilizes retained austenite to quench, but decreases its stability to tempering.

Cr, Mo, and partly V do not play a major role on the control of retained austenite, but their presence is needed for the requirements of a good bearing steel [45,46]: they present a strong carbide forming tendency that gives hardness, wear resistance, machinability, and they form efficient hardening nitrides and carbonitrides. "The reason for the large increase of hardness after carbonitriding was presented in the section Rolling Contact Fatigue Performance Enhancement Under Severe Conditions." They also increase hardenability, and lower M_S of the steel.

Mn and Ni addition, but Mn with a stronger effect, by lowering M_S and increasing hardenability, increases the stability of austenite to quench and consequently the initial retained austenite content. A too large amount of Mn (>3 vol. %) promotes twinning formation in the martensite [39], detrimental to service performance (decrease of toughness, fatigue resistance). Mn also increases the yield strength of austenite. These elements are often used for the design of stable retained austenite steels.

Si is the other element often used to control retained austenite. Some explain that Si promotes graphitization and therefore delays the formation of cementite, because in substitutional solution in ferrite, it presents strong bonds with Fe that reduce lattice vibrations and carbon diffusion [36]. It can also be explained by the following: because Si does not participate to the building of M_3C, when a carbide is formed, the Si present at that location is rejected in the vicinity of the carbide, creating a more and more impassable obstacle for carbon that slows down the carbide growth. As a consequence, additions of Si slows down carbon release from martensite for precipitation of cementite, and increase tempering resistance, thermal and mechanical softening, and retained austenite stability to tempering. It also increases hardness in annealed and hardened conditions, rendering machinability and cold forming difficult.

Alloying elements also affect retained austenite stabilization and stability through their interaction with C [39]: Mn, because it lowers M_S, discourages large scale migration of carbon; Ni and Si favor partitioning and migration of carbon to dislocations, while Mo, Cr, and Mn disfavor carbon partitioning.

Therefore, Mn, Si, and sometimes Ni are often used to design retained austenite steels on the grounds of existing through-hardening steels like SAE 52100, optimized in terms of alloy contents for bearing applications (and associated specific requirements), or carburizing or carbonitriding steels in case of case-hardening/carbonitriding heat treatments: Mn to retain austenite after heat treatment, and Si to stabilize it against thermal or mechanical ageing and keeping it in service.

Conclusions

Retained austenite is a topic discussed for years in the literature, but is still an open debate today.

Depending on the application needs, it can be considered detrimental or beneficial.

The mechanisms governing the stabilization and stability of retained austenite mentioned in the literature are discussed in this paper, and the way to use these parameters at the engineer’s benefit either to promote or suppress retained austenite is described.

In terms of dimensional stability, retained austenite can be problematic if service times and temperatures induce its transformation with resulting size changes that modify the internal clearance of bearings and their interference with the surrounding parts. The well-known microstructural mechanisms that govern these size changes and a model to predict their dimensional consequences are reviewed in this paper. This model can be used as a prediction or effect limitation tool. Industrial solutions to limit retained austenite content have been discussed, but the only efficient way to totally remove retained austenite is the selection of an appropriate tempering.

On the other hand, retained austenite can improve mechanical properties, and in bearing applications, it is known to increase RCF performance under severe conditions, and specifically under contaminated lubrication. Two material solutions are described in this paper, but the most interesting answer to contaminated lubrication is the use of a material combining both hardness for indentation resistance, and retained austenite for crack propagation resistance. That is why the use of carbonitriding of SAE 52100 that presents both characteristics (hardness and retained austenite) obtained the best results in contaminated lubrication bearing tests.

Appendix A: Model Details

All the details and hypotheses of the model can be found in Ref. [14] for the case of the martensitic heat treatment, and in Ref. [33] for the bainitic heat treatment.

The initial microstructure at $t = 0$ consists of supersaturated martensite and retained austenite (undissolved carbides are not considered). Related volume fractions and carbon concentration are indicated in **Table 3**, where f_x and $[\mathrm{C}]_x$ are respectively the volume fraction and carbon content of a phase.

FROM TEP MEASUREMENT TO PHASES VOLUME FRACTIONS AND CARBON CONTENT DURING AGEING

This step takes into account the contribution of each individual phase to the macroscopic TEP measurement at time t, through the evaluation of the reaction progress of the different phenomenon modeled by JMAK laws, and the resulting volume fraction and carbon content of the phases.

All these contributing factors are summarized in **Table 4** for martensitic heat treatments, and in **Table 5** for bainitic heat treatments, where:

Y_x = the transformed fraction described by the JMAK law,
n_x, k_x = the JMAK parameters,
f_x and $[\mathrm{C}]_x$ = respectively, the volume fraction and carbon content of a phase, and
K_x = the influence coefficient of the physical phenomenon on TEP.

The interpolation with the experimental data (TEP mastercurve at 110°C) leads to the determination of all the parameters of these laws; they are contained in **Table 6**.

FROM PHASES VOLUME FRACTIONS AND CARBON CONTENT TO MACROSCOPIC DIMENSIONAL VARIATIONS

Literal expressions used for the calculations of volume fractions and eigenstrains are gathered in **Table 7** for both heat treatments, where:

f_x = the volume fraction of phase x,
Ω_x = the lattice volume unit of phase x,
$\overline{\Omega^0}$ = the mean volume per iron atom,
X_x^Y = the molar fraction of atom Y in phase x (for carbon, derived from the weight content estimated previously $[C]_x$),
r_x = the number of iron atom in a lattice unit, and
s_x = the stoechiometry of the carbide (2.4 for ε-carbide, and 3 for Fe_3C).

TABLE 3 Volume fraction and carbon content of microstructural constituents in the initial state (t = 0)—SS stands for solid solution, and D for dislocations (notation consistent with Ref. [14]).

Phase		Volume Fraction	Carbon Content
Martensite	α'	$1 - f^0_{\gamma_R}$	$[\mathrm{C}]^0_{\mathrm{SS}}$ $[\mathrm{C}]^0_{\mathrm{D}}$
Retained austenite	γ_R	$f^0_{\gamma_R}$	

TABLE 4 Volume fraction, carbon content, reaction progress and contribution to TEP at time t of microstructural constituents for martensitic heat treatments at time t [13,14].

Phase		Volume Fraction	Reaction Progress	Carbon Content	Contribution to TEP
α''	Solid solution	$1-f^0_{\gamma_R}$		$[\mathrm{C}]_{\mathrm{SS}}=[\mathrm{C}]^0_{\mathrm{SS}}-[\mathrm{C}]_{\alpha'\to\varepsilon}-[\mathrm{C}]^{-}_{\alpha'\to\theta}$	$\Delta \mathrm{S}_{\mathrm{SS}}=\mathrm{K}_{\mathrm{C}}\left([\mathrm{C}]_{\mathrm{SS}}-[\mathrm{C}]^0_{\mathrm{SS}}\right)=-\mathrm{K}_{\mathrm{C}}()$
	Dislocations			$[\mathrm{C}]_{D\to\theta}=[\mathrm{C}]^0_{D\to\theta}Y_\theta(t)$	-
	Recovery		$Y_R(t)=1-\exp\left[-(k_R\cdot t)^{n_R}\right]$		$\Delta S_R=K_R Y_R(t)$
ε			$Y_\varepsilon(t)=1-\exp\left[-(k_\varepsilon\cdot t)^{n_\varepsilon}\right]-Y_\theta(t)$	$Y_\varepsilon(t)=1-\exp\left[-(k_\varepsilon\cdot t)^{n_\varepsilon}\right]-Y_\theta(t)$	-
$\mathrm{Fe_3C}$ (θ)			$Y_\theta(t)=1-\exp\left[-(k_\theta\cdot t)^{n_\theta}\right]$	$[C]_\theta=[C]_{\alpha'\to\theta}+[C]_{D\to\theta}$with $[\mathrm{C}]_{\alpha'\to\theta}=\left([\mathrm{C}]^0_{\mathrm{SS}}-[\mathrm{C}]^{eq}_{\alpha'\theta}\right)Y_\theta(t)$	-
γ_R		$f_{\gamma_R}=(1-Y_\theta(t))f^0_{\gamma_R}$	$Y_{\gamma_R}(t)=1-Y_\theta(t)$		
$(\alpha+\mathrm{Fe_3C})$		$f^0_{\gamma_R}-\mathrm{f}_{\gamma_R}=\mathrm{f}^0_{\gamma_R}\mathrm{Y}_\theta(\mathrm{t})$			K_{γ_R}

TABLE 5 Volume fraction, carbon content, reaction progress and contribution to TEP at time t of microstructural constituents for bainitic heat treatments [33].

Phase		Volume Fraction	Reaction Progress	Contribution to TEP
Bainite	Nanometric carbides transformation	$1-f^0_{\gamma_R}$	$Y_\theta(t)=1-\exp\left[-(k_\theta\cdot t)^{n_B}\right]$	$\Delta S_\theta=K_\theta Y_\theta(t)$
	Recovery		$Y_R(t)=1-\exp\left[-(k_R\cdot t)^{n_R}\right]$	$\Delta S_R=K_R Y_R(t)$
γ_R		$f_{\gamma_R}=(1-Y_\theta(t))f^0_{\gamma_R}$		
$(\alpha+\mathrm{Fe_3C})$		$f^0_{\gamma_R}-f_{\gamma_R}=f^0_{\gamma_R}Y_\theta(t)$		K_{γ_R}

TABLE 6 Parameters used for the model of TEP during ageing at 110°C—f = fitted, m = measured, d = obtained from the literature (from Refs. [14,33]).

Parameter	Meaning	Value for Martensitic Heat Treatment	Value for Bainitic Heat Treatment	f	m	d
k_ε	JMAK for ε-carbide	5.5×10^{-3}		✓		
n_ε	JMAK for ε-carbide	0.25		✓		
k_θ	JMAK for Fe_3C	2×10^{-6}	2×10^{-5}	✓		
n_θ	JMAK for Fe_3C	0.9	1	✓		
k_R	JMAK for recovery	10^{-12}	10^{-12}	✓		
n_R	JMAK for recovery	0.2	0.2	✓		
$[C]^0_{SS}$	Initial C content in solid solution	0.2 wt. %		✓		
$[C]^0_D$	Initial C content segregated to dislocations	0.2 wt. %				✓
$[C]^{eq}_{\alpha' \varepsilon}$	Solubility limit of with ε-carbide	0.075 wt. %		✓		
$[C]^{eq}_{\alpha' \theta}$	Solubility limit of with Fe_3C	≈0				✓
K_C	C influence coefficient on TEP	15 μV (K wt. %)$^{-1}$				✓
K_R	Recovery influence on TEP	1.5 μV K^{-1}	2 μV K^{-1}	✓		
K_θ	Nanometric carbide transformation influence on TEP		1.5 μV K^{-1}	✓		
K_{γ_R}	Austenite influence on TEP	75 nV (K vol. %)$^{-1}$			✓	
$f^0_{\gamma_R}$	Initial retained austenite content	H:10.3 vol. %	N: 4.7 vol. %		✓	
		HF: 4.7 vol. %	NF: 2.5 vol. %			

TABLE 7 Expression of volume fraction and Eigenstrain of individual phases in martensitic and bainitic heat treatments [13,14,33]. Lattice cell information gathered from Refs. [59–61].

Phase	Volume Fraction	Eigenstrain
Martensitic Heat Treatment		
α''	$f_{\alpha''} = \frac{\Omega^0_{\alpha'}/r_{\alpha'}}{\overline{\Omega_0}}\left(1 - X^C_\varepsilon s_\varepsilon - X^C_\theta s_\theta\right)\left(1 - X^{Fe^0}_{\gamma_R}\right)$ with $\overline{\Omega^0} = X^{Fe0}_{\gamma_R}\frac{\Omega_{\gamma_R}}{r_{\gamma_R}} + \left(1 - X^{Fe0}_{\gamma_R}\right)\frac{\Omega^0_{\alpha'}}{r_{\alpha'}}$ and $\Omega_{\gamma_R}(nm^3) = \left(0.3556 + 0.095X^C_{\gamma_R}/\left(1 - X^C_{\gamma_R}\right)\right)^3$	$\epsilon^T_{\alpha''} = \frac{1}{3}\ln\left(\frac{\Omega_{\alpha''}/r_{\alpha'}}{\Omega^0_{\alpha'}/r_{\alpha'}}\right)$ with $\Omega_{\alpha'} = \left(0.288664 - 0.27X^C_{\alpha'}\right)^2\left(0.288664 - 2.43X^C_{\alpha'}\right) + \Omega^0_R(1 - Y_R(t))$
ε	$f_\varepsilon = \frac{\Omega^0_{\alpha'}/r_{\alpha'}}{\overline{\Omega_0}}X^C_\varepsilon s_\varepsilon\left(1 - X^{Fe^0}_{\gamma_R}\right)$	$\epsilon^T_\varepsilon = \frac{1}{3}\ln\left(\frac{\Omega_\varepsilon/r_\varepsilon}{\Omega^0_{\alpha'}/r_{\alpha'}}\right) = 5.81\%$
Fe_3C (θ)	$f_\theta = \frac{\Omega^0_{\alpha'}/r_{\alpha'}}{\overline{\Omega_0}}X^C_\theta s_\theta\left(1 - X^{Fe^0}_{\gamma_R}\right)$	$\epsilon^T_\theta = \frac{1}{3}\ln\left(\frac{\Omega_\theta/r_\theta}{\Omega^0_{\alpha'}/r_{\alpha'}}\right) = 2.51\%$
γ_R	$f_{\gamma_R} = \frac{\Omega^0_{\gamma_R}/r_{\gamma_R}}{\overline{\Omega_0}}X^{Fe}_{\gamma_R}$ with $X^{Fe}_{\gamma_R} = \frac{f_{\gamma_R}\Omega_{\alpha'}/r_{\alpha'}}{(1 - f_{\gamma_R})\Omega_{\gamma_R}/r_{\gamma_R} + f_{\gamma_R}\Omega_{\alpha'}/r_{\alpha'}}$	$\epsilon^T_{\gamma_R} = 0\%$
($\alpha + Fe_3C$)	$f_{\alpha+\theta} = \frac{\Omega^0_{\gamma_R}/r_{\gamma_R}}{\overline{\Omega_0}}\left(1 - X^C_\varepsilon s_\varepsilon - X^C_\theta s_\theta\right)\left(X^{Fe^0}_{\gamma_R} - X^{Fe}_{\gamma_R}\right)$	$\epsilon^T_\theta = \frac{1}{3}\ln\left(\frac{\left(1 - X^C_{\gamma_R}s_\theta\right)\Omega_\alpha/r_\alpha + X^C_{\gamma_R}s_\theta\Omega_\theta/r_\theta}{\Omega_{\gamma_R}/r_{\gamma_R}}\right) = 1.38\%$
Bainitic Heat Treatment		
Recovery		$\epsilon^T_\alpha = \frac{1}{3}ln\left(\frac{\Omega^t_\alpha}{\Omega^0_\alpha}\right)$ with $\Omega^t_\alpha = 0.287^3 + \Omega^0_R(1 - Y_R(t))$ and $\Omega^0_R = 0.0001\ nm^3$
($\alpha +$ Fe_3C)		$\epsilon^T_\theta = 1.38\%$

References

[1] Zaretsky, E. V., *STLE Life Factors for Rolling Bearings*, Society of Tribologists and Lubrication Engineers, Park Ridge, IL, 1992.

[2] Averbach, B. L., Cohen, M., and Fletcher, S. G., "The Dimensional Stability of Steel: Part III. Decomposition of Martensite and Austenite at Room Temperature," *Trans. ASM*, 1948, Vol. 40, pp. 728–743.

[3] Cohen, M., "Retained Austenite," *Trans. ASM*, 1949, Vol. 41, pp. 35–94.

[4] Pearson, P. K., "Size Change of Through Hardened Bearing Steels at Application Temperatures," *SAE Trans. A*, Vol. 106, No. 2, 1997, pp. 170–175.

[5] Duval, P., Murry, G., and Constant, A., "Stabilité Dimensionnelle dans le Temps. Contribution à l'Etude des Facteurs Métallurgiques Affectant la Stabilité Dimensionnelle des Aciers," *Méc. Electr.*, Nov, 1968, pp. 28–37.

[6] Hengerer, F., Nierlich, W., Volkmuth, J., and Nutzel, H., "Dimensional Stability of High Carbon Bearing Steels," *Ball Bear. J.*, Vol. 231, 1988, pp. 26–31.

[7] Larsson, G. and Lund, T., "Prédiction de la Stabilité Dimensionnelle d'un Acier 100Cr6," *Evolution*, Vol. 2, 1999, pp. 981–987.

[8] Franklin, J., Hill, P., and Allen, C., "The Effect of Heat Treatment on Retained Austenite in a 1 % Carbon/Chromium Steel," *Heat Treat. Metals*, Vol. 6, 1979, pp. 46–50.

[9] Luty, W., "Influence of Heat Treatment on the Dimensional Stability of Bearing Rings of Steel 100 Cr 6 and 100 MnCr 6 at Room Temperature and at 150°C," *Hart. Techn. Mitt.*, Vol. 27, 1972, pp. 27–33.

[10] Murry, G., "L'Austénite Résiduelle: Quelques Rappels," *Trait. Therm.*, Vol. 349, 2003, pp. 42–49.

[11] Parrish, J., "Retained Austenite: New Look at an Old Debate," *Adv. Mater. Process.*, Vol. 145, 1994, pp. 25–28.

[12] Peilloud, F. and Guillot, M., "Contribution à l'Etude de la Stabilité Dimensionnelle des Aciers à Roulements," *Méc. Matér. Electr.*, Vol. 316, 1976, pp. 28–35.

[13] Sidoroff, C., 2002, "Analyse Microstructurale et Modélisation des Evolutions Dimensionnelles de l'Acier 100Cr6: Structures Martensitique et Bainitique," Ph.D. thesis, INSA Lyon, Lyon, France.

[14] Perez, M., Sidoroff, C., Vincent, A., and Esnouf, C., "Microstructural Evolution of Martensitic 100Cr6 Bearing Steel During Tempering: From Thermoelectric Power Measurements to the Prediction of Dimensional Changes," *Acta Mater.*, Vol. 57, No. 11, 2009, pp. 3170–3181.

[15] Yajima, E., Miyazaki, T., Sugiyama, T., and Terajima, H., "Effects of Retained Austenite on the Rolling Fatigue Life of Ball Bearing Steels," *Trans. Jpn. Inst. Metals*, Vol. 15, No. 3, 1974, pp. 173–179.

[16] Sugiura, I., Kato, O., Tsushima, N., and Muro, H., "Improvement of Rolling Bearing Fatigue Life Under Debris—Contaminated Lubrication by Decreasing the Crack Sensitivity of the Material," *ASLE Trans.*, Vol. 25, No. 2, 1982, pp. 213–220.

[17] Furumura, K., Murakami, Y., and Abe, T., “The Development of Bearing Steels for Long Life Rolling Bearings Under Clean Lubrication and Contaminated Lubrication,” *Creative Use of Bearing Steels*, *ASTM STP* 1195, J. J. C. Hoo, Ed., ASTM International, West Conshohocken, PA, 1993, pp. 285–296.

[18] Furumura, K., Murakami, Y., and Abe, T., “Case-Hardening Medium Carbon Steel for Tough and Long Life Bearing under Severe Lubrication Conditions,” *Bearing Steels into the 21st Century*, *ASTM STP* 1327, J. J. C. Hoo and W. B. Green, Jr., Eds., ASTM International, West Conshohocken, PA, 1998, pp. 285–296.

[19] Girodin, D., Ville, F., Guers, R., and Dudragne, G., “Rolling Contact Fatigue Tests to Investigate Surface Initiated Damage and Tolerance to Surface Dents,” *Bearing Steel Technology*, *ASTM STP* 1419, J. M. Beswick, Ed., ASTM International, West Conshohocken, PA, 2002, pp. 263–281.

[20] Böhmer, H.-J. and Eberhard, R., “Microstructural Optimisation of Bearing Steels for Operation Under Contaminated Lubrication by Using the Experimental Method of Dented Surfaces,” *Bearing Steel Technology*, *ASTM STP 1419*, J. M. Beswick, Ed., ASTM International, West Conshohocken, PA, 2002, pp. 244–262.

[21] Speich, G. R. and Taylor, K. A., “Tempering of Ferrous Martensites. Martensite: A Tribute to Morris Cohen,” G. B. Olson and W. S. Owen, Eds., ASM International, Materials Park, OH, 1992, pp. 243–275.

[22] Porter, D. A. and Easterling, K. E., *Phase Transformations in Metals and Alloys*, Chapman and Hall, London, 1992.

[23] Roberts, C. S., Averbach, B. L., and Cohen, M., “The Mechanism and Kinetics of the First Stage of Tempering,” *Trans. ASM*, Vol. 45, 1953, pp. 576–604.

[24] Bhadeshia, H. K. D. H., “Steels for Bearings,” *Prog. Mater. Sci.*, Vol. 57, No. 2, 2012, pp. 268–435.

[25] Cheng, L., Brakman, C. M., Korevaar, B. M., and Mittemeijer, E., “The Tempering of Iron–Carbon Martensite; Dilatometric and Calorimetric Analysis,” *Metall. Trans. A*, Vol. 19, No. 10, 1988, pp. 2415–2426.

[26] Ohmori, Y. and Sugisawa, S., “The Characterization of Carbides During Tempering of High Carbon Martensite,” *Trans. Jpn. Inst. Metals*, Vol. 12, No. 3, 1971, pp. 170–178.

[27] Tkalcec, I., Mari, D., and Benoit, W., “Correlation Between Internal Friction Background and the Concentration of Carbon in Solid Solution in a Martensitic Steel,” *Mater. Sci. Eng. A*, Vol. 442, No. 1, 2006, pp. 471–475.

[28] Speich, G. R., “Tempering of Low Carbon Martensite,” *Trans. Metall. Soc. AIME*, Vol. 245, No. 12, 1969, pp. 2553–2562.

[29] Abe, H. and Suzuki, T., “Thermoelectric Power Versus Electrical Conductivity Plot for Quench Ageing of Low-Carbon Aluminium Killed Steel,” *Trans. ISIJ*, Vol. 20, 1980, pp. 690–695.

[30] Tkalcec, I., Azcoıtia, C., Crevoiserat, S., and Mari, D., “Tempering Effects on a Martensitic High Carbon Steel,” *Mater. Sci. Eng. A*, Vol. 387, 2004, pp. 352–356.

[31] Blatt, F. J., Schroeder, P. A., Foiles, C. L., and Greig, D., Thermoelectric Power of Metals, Plenum Press, New York, 1976.

[32] Lavaire, N., Merlin, J., and Sardoy, V., "Study of Ageing in Strained Ultra and Extra Low Carbon Steels by Thermoelectric Power Measurement," *Scr. Mater.*, Vol. 44, No. 4, 2001, pp. 553–559.

[33] Tonicello, E., Girodin, D., Sidoroff, C., Fazekas, A., and Perez, M., "Rolling Bearing Applications: Some Trends in Materials and Heat Treatments," *Mater. Sci. Technol.*, Vol. 28, No. 1, 2012, pp. 23–26.

[34] Lucas, G. and Nützel, H., "Untersuchungen über die Umwandlung des Restaustenits in Niedrig Legierten Stählen mit rd. 1 C," *Arch. Eisenhütten.*, Vol. 37, No. 12, 1966, pp. 981–987.

[35] Kleber, X., Merlin, J., and Massardier, V., "La Mesure du Pouvoir Thermoélectrique: une Technique Originale de Contrôle des Alliages Métalliques," *Ed. Tech. Ingénieur*, No. RE39, 2005, pp. 1–9.

[36] Daguier, P., Baudry, G., Bellus, J., Auclair, G., Rofes-Vernis, J., Dudragne, G., Girodin, D., and Jacob, G., "Improved Bearing Steel for Applications Involving Debris, Higher Loads and Temperatures," *Bearing Steel Technology, ASTM STP* 1419, J. M. Beswick, Ed., ASTM International, West Conshohocken, PA, 2002, pp. 320–329.

[37] Zaccone, M. A. and Krauss, G., "Elastic Limit and Microplastic Response of Hardened Steels," *Metall. Trans. A*, Vol. 24, No. 10, 1993, pp. 2263–2277.

[38] Voskamp, A. P., "Material Response to Rolling Contact Loading," *J. Tribol.*, Vol. 107, No. 7, 1985, pp. 359–366.

[39] Rao, N., 1978, "Role of Quaternary Additions on Dislocated Martensite, Retained Austenite, and Properties of Iron/Chromium/Carbon,", Ph.D. thesis, University of California, Berkeley, Berkeley, CA.

[40] Lesage, J. and Iost, A., "Influence de l'Austénite Résiduelle sur la Durée de Vie en Fatigue d'Aciers Carbonitrurés," *Comptes Rendus Acad. Sci. Ser. 2*, Vol. 305, No. 2, 1987, pp. 77–80.

[41] Davis, J. R., *Surface Hardening of Steels: Understanding the Basics*, ASM International, Materials Park, OH, 2002.

[42] Chiu, Y. P. and Liu, J. Y., "An Analytical Study of the Stress Concentration around a Furrow Shaped Surface Defect in Rolling Contact," *J. Lubr. Technol.*, Vol. 92, No. 2, 1970, pp. 258–263.

[43] Daguier, P., Roesch, O., and Trojahn, W., "New Development in Through Hardened Bearing Steel Grades for Use in Contaminated Lubrication," *Bearing Steel Technology, ASTM STP* 1465, J. M. Beswick, Ed., ASTM International, West Conshohocken, PA, 2007, pp. 131–139.

[44] Tsushima, N., Maeda, K., Nakashima, H., and Kashimura, H., "New Steels Now in Use for Automotive Rolling Element Bearings," *Bearing Steels into the 21st Century, ASTM STP* 1327, J. J. C. Hoo and W. B. Green, Jr., Eds., ASTM International, West Conshohocken, PA, 1998, pp. 279–290.

[45] Nicot, C., 1994, "Etude des Mécanismes d'Endommagement d'Aciers à Roulement Sollicités en Fatigue: Effet de Défauts de Surface Simulant des Conditions de Lubrification Polluée et Rôle du Traitement Thermique," Ph.D. thesis, INSA Lyon, Lyon, France.

[46] Sarete-Cercueil, H., 1999, "Etude d'une Nouvelle Nuance d'Acier à Roulement pour Conditions d'Usage Sévères et Modélisation de son Endommagement en Présence d'une Indentation," Ph.D. thesis, INSA Lyon, Lyon, France.

[47] Shibata, M., Goto, M., Ohta, A., and Toda, K., "Development of Long Life Rolling Bearings for Use in the Extreme Conditions," *Bearing Steel Technology, ASTM STP* 1419, J. M. Beswick, Ed., ASTM International, West Conshohocken, PA, 2002, pp. 285–296.

[48] Carlson, D., Pitsko, R., Chidester, A. J., and Imundo, J. R., "The Effect of Bearing Steel Composition and Microstructure on Debris Dented Rolling Element Bearing Performance," *Bearing Steel Technology, ASTM STP* 1419, J. M. Beswick, Ed., ASTM International, West Conshohocken, PA, 2002, pp. 330–345.

[49] Luty, W. and Wyszkowski, J., "Carbonitrieren von Wälzlagerstahl 100Cr6 in Generatorslosen Gasatmosphären," *HTM*, Vol. 27, 1972, pp. 162–169.

[50] Ohki, C., "Evaluation of Scratched Contact Fatigue Life with Artificial Dent of Carbonitrided SUJ2 Steel Whose Surface Nitrogen Content is Controlled," *NTN Tech. Rev.*, Vol. 78, 2010, pp. 24–32.

[51] Rivière, A., Sarrazin, S., and Parisot, J., "Stabilisation et Vieillissement de l'Austénite dans Divers Aciers, entre 25 et 80°C," *Mem. Sci. Rev. Metall.*, Vol. 70, No. 10, 1973, pp. 739–745.

[52] Leslie, W. C. and Miller, M. R., "The Stabilization of Austenite by Closely-Spaced Boundaries," *Trans. ASM*, Vol. 57, 1964, pp. 972–979.

[53] Meyzaud, Y. and Sauzay, C., "Prévision des Pourcentages D' Nospace Austéniterésiduelle à l'Aide des Courbes de Transformation en Refroidissement Continu des Aciers," *Mem. Sci. Rev. Metall.*, Vol. 69, 1972, pp. 763–774.

[54] Li, L., Wollants, P., He, Y. L., DeCooman, B. C., Wei, X. C., and Xu, Z. Y., "Review and Prospect of High Strength Low Alloy TRIP Steel," *Acta Metall. Sin. (Engl. Lett.)*, Vol. 16, No. 6, 2009, pp. 457–465.

[55] Riedel, J., "Retained Austenite and Dimensional Stability," *Metal Prog.*, Vol. 88, No. 3, 1965, pp. 78–82.

[56] Murry, G., "La Stabilité Dimensionnelle des Aciers après Traitements Thermiques—Aspects Métallurgiques," *Trait. Therm.*, Vol. 128, 1978, pp. 43–50.

[57] Lymann, J., "High Carbon Steel Microcracking During Hardening," *J. Eng. Mater. Technol.*, Vol. 106, No. 3, 1984, pp. 253–256.

[58] Beswick, J. M., "Fracture and Fatigue Crack Propagation Properties of Hardened 52100 Steel," *Metall. Mater. Trans. A*, Vol. 20, No. 10, 1989, pp. 1961–1973.

[59] Hirotsu, Y. and Nagakura, S., “Crystal Structure and Morphology of the Carbide Precipitated from Martensitic High Carbon Steel during the First Stage of Tempering,” *Acta Metall.*, Vol. 20, No. 4, 1972, pp. 645–655.

[60] Bagaryatskii, Y. A., “Possible Mechanism of Martensite Decomposition,” *Dokl. Acad. Nauk. SSSR*, Vol. 73, 1950, pp. 1161–1164.

[61] Cheng, L., Böttger, A., De Keijser, T. H., and Mittemeijer, E. J., “Lattice Parameters of Iron–Carbon and Iron–Nitrogen Martensites and Austenites,” *Scr. Metall. Mater.*, Vol. 24, 1990, No. 3, pp. 509–514.